ORGANIC PROCESS RESEARCH & DEVELOPMENT
OPR&D

pubs.acs.org/OPRD Article

From Milligram to Kilogram Manufacture of AZD4573: Making It Possible by Application of Enzyme-, Iridium-, and Palladium-Catalyzed Key Transformations

Staffan Karlsson,* Helen Benson, Calum Cook, Gordon Currie, Jerome Dubiez, Hans Emtenäs, Janet Hawkins, Rebecca Meadows, Peter D. Smith, and Jeffrey Varnes

Cite This: https://doi.org/10.1021/acs.oprd.1c00058 Read Online

ACCESS | Metrics & More | Article Recommendations | Supporting Information

ABSTRACT: With the first generation medicinal chemistry synthesis as a starting point, we describe herein process development of **AZD4573**, an oncology drug candidate. In addition to improved yields and removal of chromatographic steps, we have addressed other factors such as availability of starting materials as well as safety of the chemistry involved. With several steps involving volatile, reactive, and non-UV active materials, reaction optimization was facilitated by implementing off-line ^{1}H NMR analysis of crude mixtures. Key transformations targeted for process development included a Wolff–Kishner reduction, an iridium-catalyzed borylation, and enzymatic resolution of a racemic amino-ester.

KEYWORDS: *iridium borylation, enzymatic resolution, acetylation, Suzuki, Wolff–Kishner, ammonolysis*

INTRODUCTION

Cyclin-dependent-kinases (CDKs) are members of the Ser/Thr family and are classified into two groups: those involved in cell cycle control and those involved in transcription regulation/RNA processing. Loss of cell cycle control through deregulation of CDK activity is a key aspect of tumorigenesis. Cyclin-dependent-kinase 9 (CDK9) is one of the most studied transcriptional CDKs, the inhibition of which induces apoptosis in a variety of cell lines and antitumor efficacy *in vivo* through transcriptional downregulation of short-lived proteins such as MCL-1.[1,2] We recently reported the discovery of CDK9 inhibitor **AZD4573**, which is currently in Phase 1 for hematological malignancies.[3]

Retrosynthetically, **AZD4573** can be obtained from the three key building blocks **A**–**C** via a Suzuki reaction and an amide coupling, respectively (Figure 1). For large scale applications, while the convergent strategy used by the medicinal chemists to achieve the synthesis of **AZD4573** was appealing, the routes to produce the various building blocks were not straightforward for scale-up. Therefore, despite the need for rapid delivery of API for both preclinical and clinical studies, we devoted time to identify alternative routes and optimal conditions for assembly of building blocks **A**–**C**.

The detailed synthesis of **AZD4573** used by medicinal chemistry (referred to as the first-generation synthesis) is depicted in Scheme 1. Boronate building block **6** was prepared in six steps starting with alkylation of pyrazole with commercially available ethyl ester **1** in DMA using cesium carbonate as base. After purification by chromatography, hydrolysis with sodium hydroxide and filtration/trituration with aqueous acid (pH 3) afforded acid **2**. Following thorough drying, **2** was treated with 2 equiv of *n*-butyllithium (not titrated) in 2-methyltetrahydrofuran to afford diaza-bicycle **3** in moderate yield. A Wolff–Kishner reduction provided the known compound **4**,[4] and after treatment with either NBS or NIS, building block **5** was obtained. This was followed by palladium-catalyzed borylation to give **6**, which was purified by chromatography.

Building block **8** was either purchased or could be prepared from 2-fluoropyridine **7** through ammonolysis in the presence of concentrated aqueous ammonium hydroxide under microwave conditions to afford the corresponding 2-aminopyridine **8** in excellent yield after ion-exchange chromatography. Building block **10** was obtained in a three-step process from commercially available racemic amino acid **9**.[5] Acid **10** was coupled with **7** using Ghosez's reagent to afford **11** in moderate yield. Suzuki coupling of **6** with **11** using second Generation XPhos precatalyst was followed by chromatography to provide **12**. Deprotection under acidic conditions, purification of the resulting amine by ion-exchange chromatography, and acetylation with acetic anhydride using either pyridine or triethylamine as base then gave **AZD4573** (after chromatography) in moderate yield.

Although the route in Scheme 1 was efficient in terms of rapid synthesis of compound libraries for evaluation of candidate drugs, for application toward kilogram scale supply of **AZD4573** we needed to address concerns regarding safety, solubility, and purification. We therefore investigated route modifications and alternatives based on the following assessments:

Special Issue: Excellence in Industrial Organic Synthesis 2021

Received: February 16, 2021

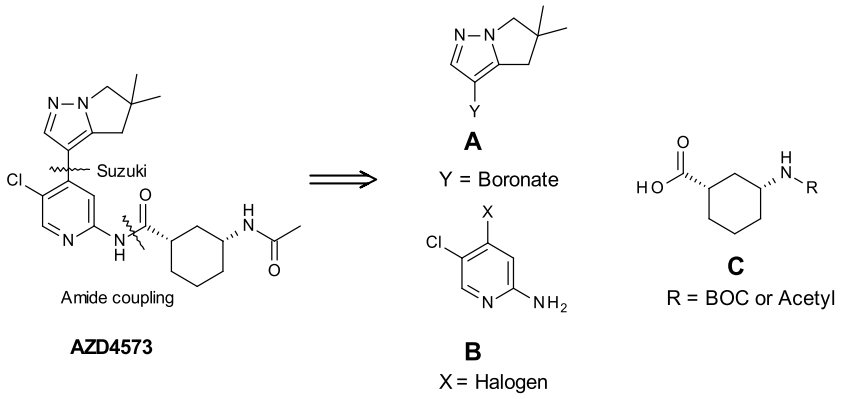

Figure 1. Retrosynthetic disconnection of **AZD4573**.

Scheme 1. First Generation Synthesis of AZD4573 (Purification Methods Are Italicized)

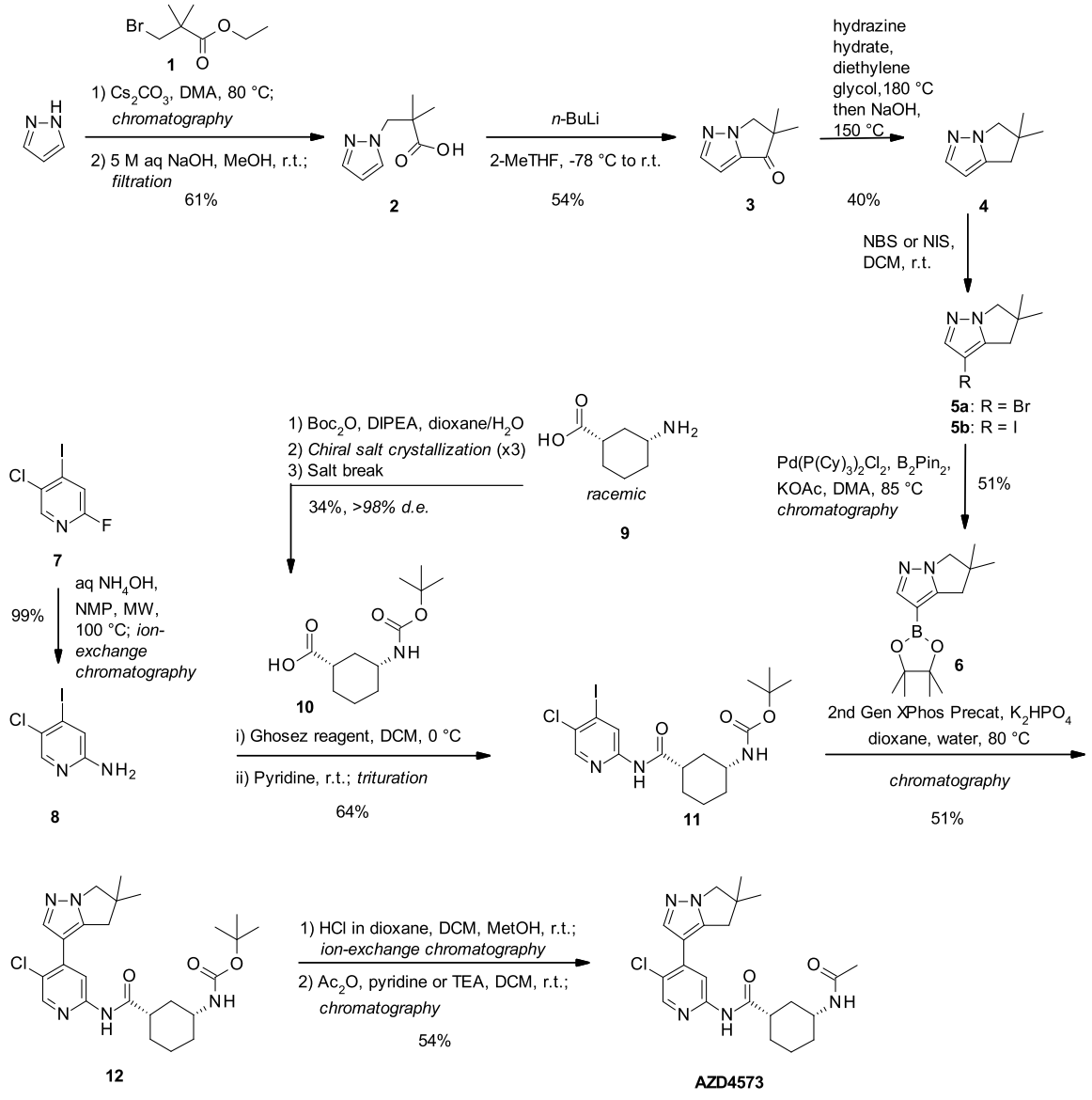

(i) A Suzuki coupling very late in the synthetic route resulted in unacceptable levels of residual palladium in final API. A change in order of the steps might also have a favorable outcome on the solubility of intermediates.

(ii) The ammonolysis of the fluoropyridine **7** constituted a hazardous operation.

(iii) Although the Wolff–Kishner reduction of **3** could be used for large scale manufacture, a more efficient catalytic method was desirable.

https://doi.org/10.1021/acs.oprd.1c00058
Org. Process Res. Dev. XXXX, XXX, XXX−XXX

Scheme 2. Comparison of the First Generation Synthesis of BPin Ester 6 (Method A and B) with the Second Generation Synthesis (Method C)

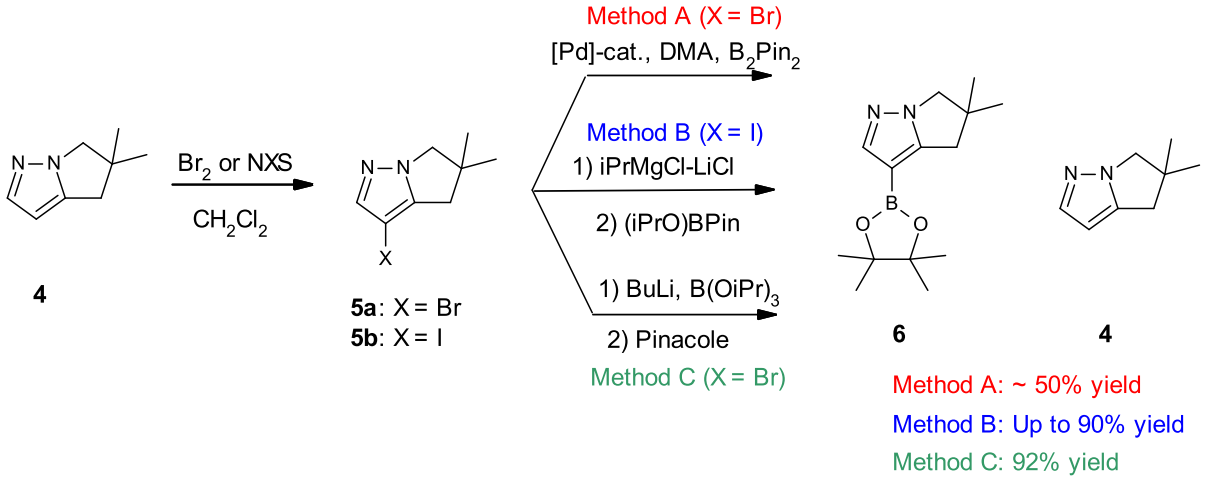

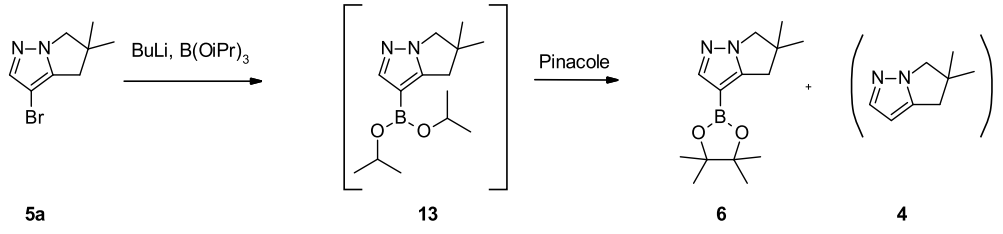

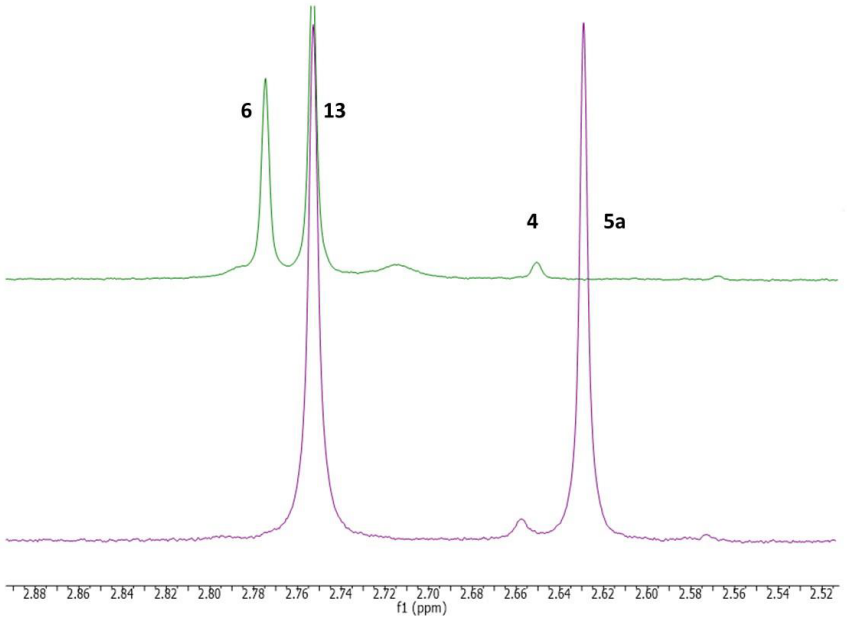

Figure 2. ^{1}H NMR recording in $CDCl_3$ of the crude mixture of (i) lithium−halogen exchange of **5a**/triisopropylborate formation **13** (purple) and (ii) pinacole trans-esterification to **6** (green).

(iv) Racemic amino acid **9** was only available in limited quantities.
(v) The Pd-catalyzed borylation of compound **5** was inefficient and low yielding, mainly due to proto-dehalogenation as a side reaction.
(vi) Several steps included chromatography for purification of intermediates. We aimed for a process where crystallizations could be employed instead.
(vii) The highly reactive Ghosez reagent used for the amide coupling is not accessible in large quantities, and handling is nontrivial.
(viii) We believed that the removal of the BOC group of **12** followed by acetylation added two unnecessary steps to the sequence, and we wanted to evaluate an alternative convergent strategy where the acetyl group could function also as a protecting group.

https://doi.org/10.1021/acs.oprd.1c00058
Org. Process Res. Dev. XXXX, XXX, XXX−XXX

In the following sections, we describe our efforts to address the aforementioned issues identified in the first generation synthesis and the development of a route (referred to as the second generation synthesis) to prepare multigram quantities of **AZD4573** to support preclinical studies. We also describe the development of a third generation synthesis used to manufacture kilogram quantities of **AZD4573** for clinical studies.

RESULTS AND DISCUSSION

Development of a Large Scale Route to Pyrazole Fragment (A). *Second Generation Synthesis of* ***6****.* For the initial scale-up development of **AZD4573** we decided to continue with use of the Wolff−Kishner conditions for reduction of **3** and focused our efforts on finding better conditions for the borylation of **5**, which, in the first generation synthesis, had a moderate yield mainly due to the formation of up to 50% of byproduct **4** as a result of hydrodehalogenation (Method A, Scheme 2). Metalation of **5b** (Method B, X = I, Scheme 2) had been investigated by the medicinal chemistry team, and while this had been demonstrated to be feasible (yields up to 90% achieved), the results were inconsistent and varied according to scale.

As a first step we sought to identify optimized conditions for both the formation and subsequent borylation of bromide **5a**, aiming to improve atom efficiency, yield, and waste profile for the overall conversion of pyrazole **4** to BPin ester **6**. On a small scale, we found that bromination of **4** using bromine in slight excess furnished compound **5a** in good isolated yield (85%). However, using NBS as reagent gave a much cleaner profile and a faster rate of reaction. Next, inspired by recent publications which described the use of triisopropylborate in lithium exchange−borylation reactions, we planned to apply a similar strategy for our substrate **5a**.[6] The reaction is based on an *in situ* formation of an isopropylborate intermediate which is trans-esterified to the desired pinacol boronate using pinacole. Before we were ready to attempt such a strategy we needed a good analytical tool to be able to monitor all possible intermediates and byproducts formed during the reaction course. The low UV-absorbance, volatility, and reactivity of the intermediates made it difficult to use traditional methods like HPLC and GC. Instead, we chose to use off-line ^{1}H NMR analysis for this study and were pleased to see that well separated peaks were obtained for the compounds/intermediates of interest (Figure 2).

Optimal results were obtained using cryogenic conditions (−70 °C) where triisopropylborate was present from the start of reaction prior to addition of butyllithium. Using such conditions resulted in significantly less proto-debromination which generates **4**. Also, an excess of ∼1.8 equiv of the triisopropylborate was required to efficiently inhibit this side-reaction. To reach full conversion to intermediate **13** it was also necessary to use an excess of butyllithium[7] (∼1.5 equiv). These results were in line with those reported by Stewart et al. using an analogous compound.[6] Using these optimal conditions we performed the reaction on a > 100g scale with consistent results and only trace amounts of byproduct **4** were detected. Next, an *in situ* trans-esterification of the isopropylborate ester intermediate **13** with pinacol was performed resulting in the desired pinacole ester **6**. This reaction was also easily monitored by ^{1}H NMR of the crude mixture (Figure 2), and we found that several hours at 20 °C were required to reach full conversion. A simple workup consisting of aqueous washes followed by concentration gave pinacole ester **6** in 64% purity (w/w) by ^{1}H NMR (92% yield). Major impurities were pinacol and some residual toluene. These contaminants did not interfere in the subsequent Suzuki coupling, and therefore we chose not to spend time optimizing this reaction further.

Third Generation Synthesis of 6, Addressing the Hazardous Wolff−Kishner Reduction. For future larger scale manufacture to support clinical studies, we believed that employing a low yielding batchwise Wolff−Kishner reduction of **3**, as used in the first and second generation synthesis, would not be a first choice method for this transformation. Therefore, in parallel to the ongoing work to manufacture **4** using the existing Wolff−Kishner batch-wise process, a continuous flow approach was investigated.[8] Also a catalytic hydrogenation approach was attempted as an alternative reduction method (Scheme 3).

Scheme 3. Alternative Strategies To Reduce 3 to Compound 4

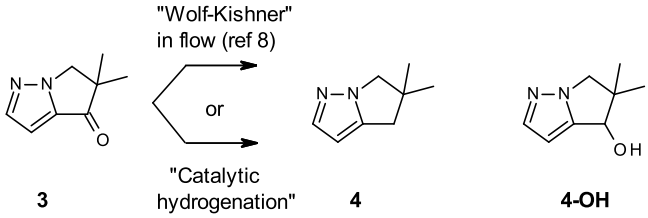

The chief concerns in the catalytic hydrogenation approach were (a) incomplete reduction leading to formation of secondary alcohol **4-OH** and (b) reduction of the pyrazole ring.

We found that the quality of the starting material **3** was crucial in order to have a positive hydrogenation outcome. Less pure starting material frequently gave lower yields or no conversion, and it was assumed that this was due to poisoning of the catalyst by contaminants. Starting from high quality **3** (95 wt %/wt), use of the highly active commercially available Johnson-Matthey 5% Pd/C paste catalysts 5R39 and 5R87L provided immediate hits for complete conversion of **3** to the partially reduced alcohol **4-OH** (Table 1, entries 1−8). Based on these promising results a reactivity screen was initiated, using the JM 5% Pd/C 5R39 catalyst in the presence of strong acid additives (MsOH, TFA, and H_2SO_4) at elevated temperatures. It was then found that, at temperatures of 80 °C and above, the desired conversion to **4** started to occur, with the best conversions obtained with high catalyst loading (entry 11). Above 120 °C, a breakdown in the reaction progression (potentially due to sintering of the catalyst) and additional byproducts (including pyrazole reduction) started to manifest (entry 12). Finally, concentration screening at the optimal temperature of 120 °C revealed that increasing the concentration of the reaction, from 33.3 rel vol H_2O to 10 rel vol H_2O, achieved the target profile of >90% conversion to desired compound **4** with <5% byproducts (entries 14 and 15).

Overall, the screening demonstrated that catalytic hydrogenation (3 barg H_2) of **3** in water (10 rel vol) using 150 wt % of the 5% Pd/C catalyst 5R39 under strongly acidic conditions (1.25−1.50 equiv of H_2SO_4) at 120 °C furnished the desired compound **4** with an acceptable crude purity profile.

We believe that, with further appropriate development and optimization, this alternative approach of reduction would have great potential as a viable large-scale route. However, the strongly acidic conditions used, in combination with the high temperature, would require pressurized reactors with a strong tolerance to these harsh conditions. Reluctantly, due to the specialized nature of such equipment and the ongoing time

https://doi.org/10.1021/acs.oprd.1c00058
Org. Process Res. Dev. XXXX, XXX, XXX−XXX

Table 1. Screening of Conditions for Hydrogenation of 3 to 4[a]

					% HPLC Area			
Entry	Cat. loading (%wt/wt)	Additive (equiv)	Concn (rel vol H_2O)	Temp (°C)	3	4	4-OH	Other[b]
1	50	MsOH (2.50)	33.3	60	0.0	0.0	99.2	0.8
2	50	MsOH (1.25)	33.3	60	0.0	0.0	97.7	2.3
3	50	TFA (2.50)	33.3	60	7.8	0.0	91.4	0.8
4	50	TFA (1.25)	33.3	60	1.1	0.0	98.3	0.6
5	50	H_2SO_4 (2.50)	33.3	60	0.0	0.0	99.2	0.8
6	50	H_2SO_4 (1.25)	33.3	60	0.0	0.0	99.4	0.6
7	50	H_2SO_4 (1.25)	33.3	80	0.6	0.8	97.9	0.7
8	50	H_2SO_4 (1.25)	33.3	100	0.0	6.9	88.6	4.5
9	50	H_2SO_4 (1.25)	33.3	120	0.9	29.8	64.8	4.4
10	100	H_2SO_4 (1.25)	33.3	120	0.4	80.3	18.1	1.3
11	150	H_2SO_4 (1.25)	33.3	120	0.3	92.0	6.6	1.1
12	50	H_2SO_4 (1.25)	33.3	140	65.0	17.1	0.0	17.9
13	150	H_2SO_4 (1.50)	33.3	120	0.0	92.4	6.9	0.7
14	150	H_2SO_4 (1.25)	10	120	0.0	91.9	4.4	3.7
15	150	H_2SO_4 (1.50)	10	120	0.2	92.4	4.9	2.5

[a]The high throughput screening was performed in a Biotage Endeavor (8 reactor array). Catalyst and substrate **3** (90 mg) were charged, followed by water and acid additive. The reactors were purged with nitrogen 3 times and H_2 3 times followed by hydrogenation under 3 barg of hydrogen at the temperature stated in Table 1 for 16 h. The mixtures were centrifuged and aliquoted and analyzed by GC/MS, HPLC and ^{1}H NMR. [b]Combined impurity fractions, including reduction of pyrazole ring.

Table 2. High-Throughput Screening for Direct Ir-Catalyzed Borylation of 4[a]

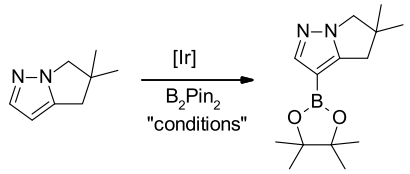

4 **6**

						Conversion of **4** to **6** (% UPLC)		
Entry	[Ir]-cat. (mol %)	ligand[b]	mol %	solvent	temp (°C)	1 h	3 h	23 h
1	2.5	tmphen	5	hexane	60	28	68	100
2	2.5	tmphen	5	THF	60	34	81	100
3	2.5	tmphen	5	iPrOAc	60	40	98	99
4	2.5	tmphen	5	CPME	60	36	91	100
5	2.5	tmphen	5	EtOAc	60	15	72	72
6	2.5	tmphen	5	MeTHF	60	32	74	100
7	2.5	tmphen	10	hexane	60	34	72	100
8	2.5	tmphen	10	THF	60	29	88	100
9	2.5	tmphen	10	MTBE	60	40	76	100
10	2.5	tmphen	10	MeTHF	60	30	72	100
11	2.5	tmphen	10	CPME	60	41	98	100
12	2.5	tmphen	10	iPrOAc	60	40	97	98
13	1	tmphen	4	hexane	80	49	88	100
14	1	tmphen	4	THF	80	77	100	100
15	1	tmphen	4	CPME	80	82	100	100
16	1	tmphen	4	MeTHF	80	58	99	100

[a]$[Ir(cod)OMe]_2$ (1–5 mol %), ligands (4–10 mol %), B_2pin_2 (1.5 equiv), and internal standard were charged to reaction vials in an inerted glovebox (<5 ppm of O_2 and <1 ppm of H_2O). Solvent (0.85 mL) and **4** (0.2 mmol as a 1.86 M solution in hexane) were then added, and the vials were sealed, stirred, and heated for 23 h. [b]tmphen = 3,4,7,8-tetramethylphenanthroline.

constraints to manufacture API for the initial clinical studies, we did not pursue further this new hydrogenation strategy, nor the continuous Wolff–Kishner approach mentioned above. Instead it was decided to revert to the previously employed Wolff–Kishner batch conditions to support the project with the building block **4**.

Investigating an Iridium Catalyzed Borylation Approach To Obtain 6. Although the lithium–halogen exchange/borylation sequence in the second generation synthesis was efficient in terms of yield and ease of workup, for further scale-up we were concerned about the cryogenic conditions required. Furthermore, a direct access to pinacole ester **6** where the bromination step could be excluded was appealing. Inspired by successful iridium catalyzed borylations of various arenes in the literature, which are applicable also on a large scale, this led us to attempt a similar strategy (Table 2).[9]

https://doi.org/10.1021/acs.oprd.1c00058
Org. Process Res. Dev. XXXX, XXX, XXX–XXX

From our initial condition screening (see Supporting Information, Table 1), we could clearly see that direct borylation of **4** using 5 mol % of $[Ir(cod)OMe]_2$ as the catalyst looked promising. Other than with highly polar solvents such as DMF and DMSO, the desired borylated product **6** was produced with conversions ranging from moderate to excellent at the 1 h sample point. Selecting tmphen as the preferred ligand a more extensive screen was performed to identify optimal solvent and conditions (Table 2). It was found that ethers and other nonprotic solvents gave full conversion to **6** within 23 h, and that by increasing the reaction temperature from 60 to 80 °C, a low catalyst loading of 1 mol % was sufficient to reach full conversion within this reasonable time frame. Using the conditions of entry 14 with no additional optimization, we found that the reaction gave consistent and good results and these conditions were successfully applied on multikilogram scale.

Development of a Large Scale Route to Aminopyridine Fragment (B). Upon planning for future large scale campaigns we sought suppliers of both the fluoro compound **7** and the aminopyridine **8** (Scheme 4).

Scheme 4. Ammonolysis of Compound 7

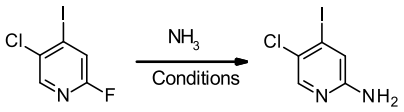

7 **8**

It was found that aminopyridine **8** was not readily accessible in large quantities from commercial sources. The fluoropyridine on the other hand was easy to access from various suppliers. Therefore, we purchased fluoropyridine **7** and devoted our time in optimizing the ammonolysis of this compound. Intrinsic to ammonolysis of fluoropyridines are several potential hazards such as (i) exposure to toxic and volatile ammonia (ii) pressurized vessels at a high temperature, (iii) incompatibility of ammonia with organic solvents and (iv) formation of etching hydrogen fluoride that might damage reactor equipment. In the first generation synthesis, the ammonolysis was performed at 100 °C in a MW vial using a large excess of ammonia in an organic cosolvent such as NMP. This was followed by purification of the product **8** by ion-exchange chromatography. We believed that a similar strategy could be used also for large scale applications but where most of the aforementioned issues were addressed. We also aimed for a chromatography-free process, and we wanted to avoid the dependence upon microwave conditions.

*Second Generation Synthesis of **8**.* To start with, we screened various thermal conditions for the ammonolysis in sealed microwave vials by varying the organic cosolvent and also the loading of ammonia (Table 3).

A cleaner profile and a better conversion was obtained when performing the reactions using aqueous ammonia and a cosolvent such as DMSO or NMP (entries 4−8). Ammonia in alcoholic solvents such as ethanol gave rise to byproducts, and these reactions were also slow (entries 1 and 2). One major drawback when using a combination of organic solvent and aqueous ammonia was that, upon mixing, an exothermic reaction occurred and severe foaming was also observed which was expected to be troublesome to control on a large scale. Also, the heat generated during mixing resulted in loss of ammonia. To circumvent these problems, attempts were made to perform the reaction under continuous processing (Figure 3).

Thus, starting material **7** was dissolved in NMP and mixed in a simple T-piece with aqueous ammonia followed by reaction at 100−140 °C in a coiled PFA tubing reactor. Unfortunately, very low conversions were obtained and, given the time required to reach full conversion, this process was deemed inefficient. Under the strict time constraints given to deliver API for initial preclinical studies, we chose to use a batch approach to manufacture **8** which we considered safe at this scale despite the aforementioned issues.

On 100 g scale in a steel vessel at 100 °C and using aqueous ammonia (13 equiv) in NMP as solvent, fluoropyridine **7** underwent ammonolysis to give, after extraction and concentration, aminopyridine **8** in 93% assayed yield by ^{1}H NMR as a highly discolored solid. Although we initially were concerned about the generation of HF and its corrosive/etching properties, we did not visually observe any damage to the reaction vessel, probably due to the large excess of ammonia used.[10] To avoid the need for chromatography for purification of **8**, a quick screen of suitable solvents for crystallization was performed. Here we found that the use of toluene gave the pure colorless crystalline compound **8** in 65% assayed yield. For further scale-up, we planned to do a more rigorous safety evaluation and find better conditions for the ammonolysis reaction.

*Third Generation Synthesis of **8**.* Accommodation of the ammonolysis reaction (Scheme 5) at the kilogram scale required careful consideration of chemical process hazard data with the equipment capability in mind. In this case, a jacketed pressure vessel constructed of C22 hastelloy having a working pressure of up to 10 barg was used. A controlled addition of the 5-chloro-2-fluoro-4-iodopyridine in NMP solution to the 28 wt % ammonia

Table 3. Ammonolysis of Fluoropyridine 7[a]

entry	solvent	cosolvent	NH_3 (equiv)	temp (°C)	time	conv[b]	comment
1	EtOH	–	5	100	20 h	46%	byproducts
2	EtOH	–	12	80	72 h	60%	–
3	water	–	30	80	20 h	70%	byproducts
4	water	NMP (55%)	15	80	20 h	100%	clean
5	water	DMSO (55%)	15	80	20 h	97%	clean
6	water	THF (55%)	15	80	20 h	50%	clean
7	water	NMP (55%)	10	70	20 h	100%	clean
8	water	NMP (40%)	13	100	20 h	100%	clean

[a]The reactions were performed in sealed microvials (0.1 g substrate/1 mL solvent) and heated in an oil bath. [b]Conversion of **7** determined by HPLC.

https://doi.org/10.1021/acs.oprd.1c00058
Org. Process Res. Dev. XXXX, XXX, XXX−XXX

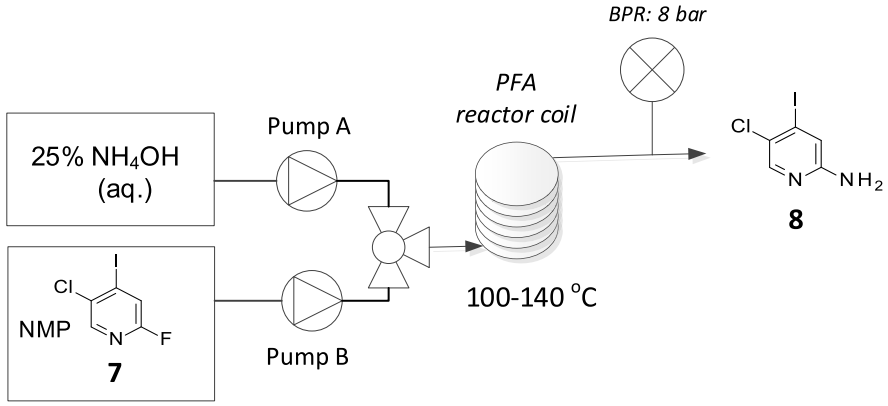

Figure 3. Attempted continuous ammonolysis of 7.

Scheme 5. Ammonolysis of 7 Using a Two-Stage Temperature Ramping

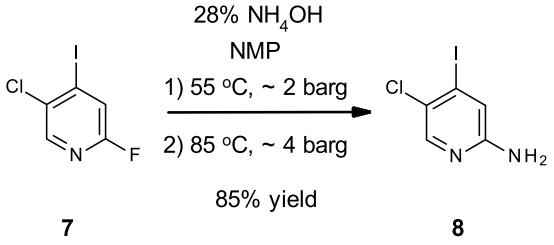

solution at ambient temperature with efficient agitation ensured good control of the mixing exotherm. However, prior assessment of the "all in" reaction exotherm had indicated that, for the heat of reaction of 156 kJ/mol 5-chloro-2-fluoro-4-iodopyridine and operating at a reaction temperature of 90 °C with the vessel vent closed, an adiabatic temperature rise to ca. 130 °C could occur, resulting in an associated pressure of 13.8 barg and hence a vessel overpressure scenario. The reaction conversion, process temperature, and pressure relationship was explored further, based on taking a two-stage temperature approach to the reaction. The mixture of 7 in 28% NH_4OH (aq.) and NMP would be held at ~50 °C until a conversion of at least 60% was reached prior to increasing the temperature to ~85 °C to complete the reaction (Scheme 5). Modeling of this two-stage approach indicated that the temperature rise caused by the reaction exotherm in a loss of vessel cooling event would be insufficient to cause vessel overpressure. Thus, an inherent safety approach for the accommodation was achieved. Figure 4a shows the predicted pressure drop for the reaction hold at 55 °C and then the actual trend from the plant data historian for the hold. The former is with respect to reaction conversion, and the actual data are recorded with time, as it was not possible to monitor reaction conversion during the hold. Figure 4b shows pressure data with time from the plant data historian for the second reaction temperature step to 85 °C and hold.

Development of a Large Scale Route to Amino Acid Fragment (C). *Second/Third Generation Synthesis of 15.* While the homochiral building block **C** (R = BOC) was commercially available, we decided that the limited accessibility made commercial sourcing an undesirable strategy to cover the supply needs for both preclinical and initial clinical trials. Although the compound can easily be prepared in enantiopure form by following published procedures, these are based on repeated crystallization with homochiral amines in low overall yield.[5] Therefore, we wanted to investigate other routes to this compound, and as such, two strategies were evaluated (Scheme 6):

(1) Enzyme catalyzed enantioselective hydrolysis of racemic esters (Strategy 1)
(2) Enzyme catalyzed enantioselective acetylation of racemic amino-ester rac-**14** (Strategy 2)

Literature reports describe the efficient resolution of BOC protected amino-esters by employing various lipases to give enantiopure protected amino acids such as **C**.[11] We began to investigate such an approach and in parallel to that work we also spent time on the acetylation/resolution of *rac*-**14** (strategy 2) which, if successful, would provide the additional advantage of removing the need for the additional Boc-deprotection/acetylation sequence used in the first generation synthesis of **AZD4573**. There are several examples of enantioselective acylations of racemic primary amines in the literature, and in particular the immobilized Candida Antarctica lipases such as Novozym435 have been successfully employed.[12] We were pleased to find that in our case, using Novozym435 as the lipase and either EtOAc or iPrOAc as the solvent/acetyl donor, an efficient resolution of a racemic mixture of **14** was obtained furnishing, after subsequent crystallization and hydrolysis, amidoacid **15** in >99% ee.[13] With some further optimization and development of this approach we have established a viable route suitable for multikilogram manufacture of **15** in 32% overall yield from *rac*-**14**. With this new building block in hand, a subsequent deprotection/acetylation strategy after amide coupling, as used in the first generation synthesis of **AZD4573**, was not needed.

AZD4573 Route Strategy: Assembly of Building Blocks A−C. To assemble the three building blocks **A**−**C**, two options are available. Either **B** can be coupled with **C** to give **BC** followed by coupling with **A** to give **AZD4573** or a coupling of **A** with **B** to give **AB** followed by coupling with **C** would give the same compound (Figure 5). Both of these strategies were evaluated and the factors that were taken into consideration were (i) physical properties and ease of handling of **BC** vs **AB**, (ii) palladium content in final API **AZD4573**, and (iii) cost and accessibility of **A** vs **C**.

We found that intermediate **BC** had very unfavorable properties compared with **AB** and resulted in a troublesome extractive workup due to low solubility. This also led to a low yield in the subsequent Suzuki coupling. A Suzuki coupling as the final step also was unfavorable in terms of risk of contamination of final API with unacceptable levels of

https://doi.org/10.1021/acs.oprd.1c00058
Org. Process Res. Dev. XXXX, XXX, XXX−XXX

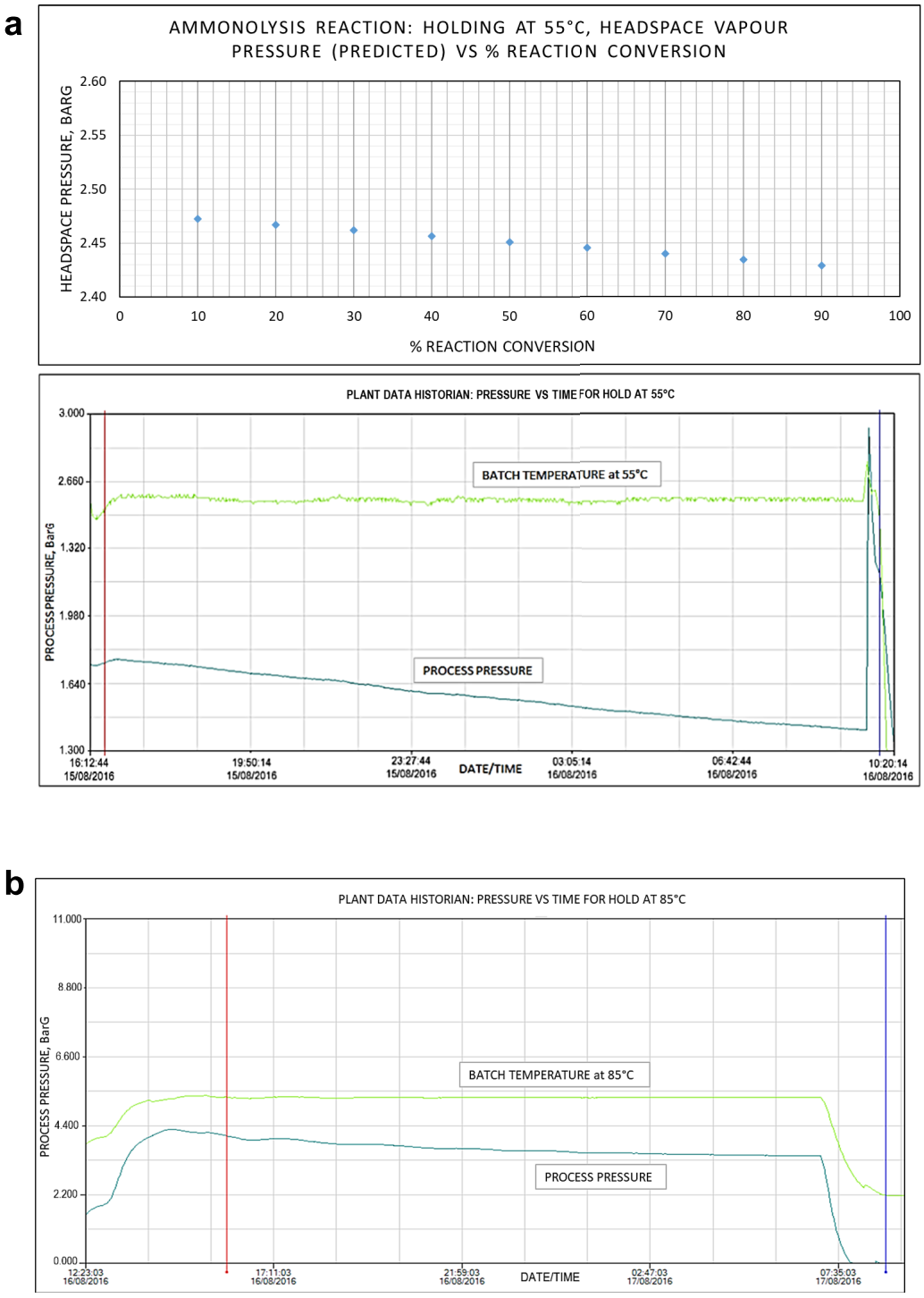

Figure 4. (a) Predicted pressure drop vs conversion for the ammonolysis reaction hold at 55 °C and actual pressure drop vs time for the reaction hold at 55 °C. (b) Actual pressure vs time for the second reaction hold at 85 °C.

palladium. This would require substantial amounts of scavenger to reduce levels of Pd to an acceptable level. These disadvantages should of course be balanced against the relative cost of building block **A** vs **C**. We considered **A** to be of higher value than **C** because of the recent development of the cost-effective enzyme catalyzed acetylation/resolution strategy which could be used for multikilogram manufacture of **C**. However, because of the aforementioned issues with the **BC** intermediate and the nonfavorable strategy to implement a palladium catalyzed reaction as the last step in the synthesis of **AZD4573**, we chose to use an approach where we first coupled **A** with **B** via a Suzuki reaction followed by an amide coupling with **C** to give **AZD4573**. In the next sections we describe our efforts in developing good large scale methods for these two transformations.

Optimization of Suzuki Reaction. Although a good yield in the Suzuki coupling was obtained in the first-generation synthesis, for cost reasons, the excess of **A** required (110−150 mol %) to reach full conversion of **B** was of major concern. Also, we wanted to replace the chromatography employed in the first

https://doi.org/10.1021/acs.oprd.1c00058
Org. Process Res. Dev. XXXX, XXX, XXX−XXX

Scheme 6. Two Potential Strategies To Obtain Homochiral Building Block C

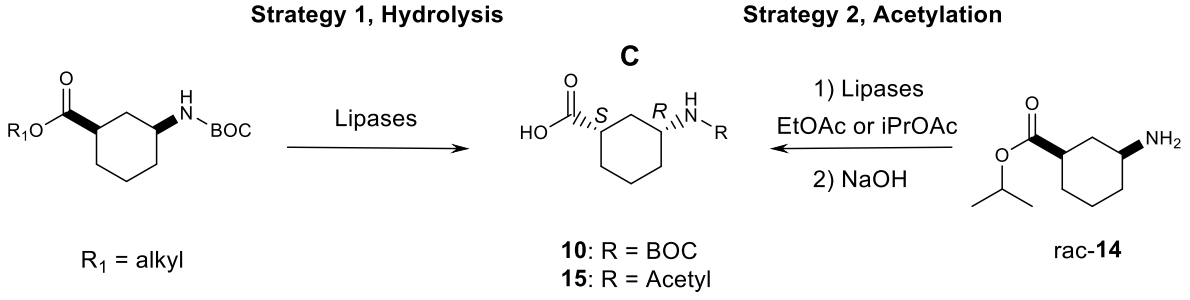

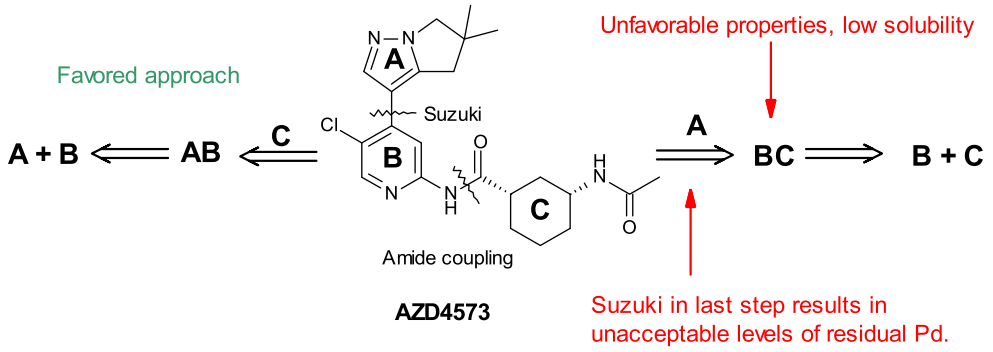

Figure 5. Strategies to assemble the three building blocks **A**, **B**, and **C**.

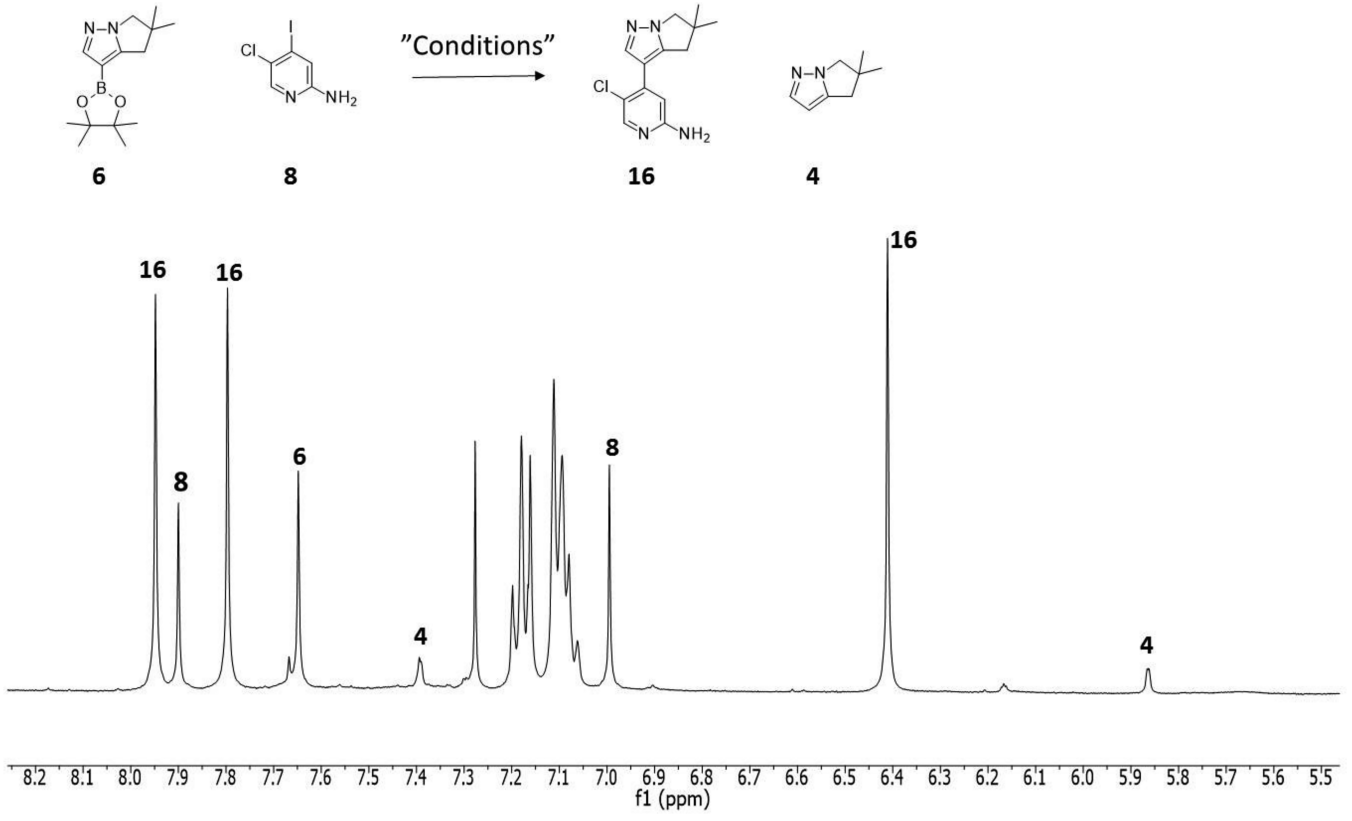

Figure 6. ^{1}H NMR recorded of the crude Suzuki mixture in $CDCl_3$.

generation synthesis with crystallization. Furthermore, we wanted to avoid the use of the solvent 1,4-dioxane, which easily forms peroxides, and also identify a less expensive base relative to K_2HPO_4 used in the first generation synthesis. To find optimal conditions, a good understanding of the reaction and the kinetics as well as potential side reactions is of great value. Therefore, we searched for an analytical technique where this could be achieved. Due to the volatile nature and low UV-absorbance of some of the intermediates, we chose to use off-line ^{1}H NMR monitoring as an analytical tool for this reaction

https://doi.org/10.1021/acs.oprd.1c00058
Org. Process Res. Dev. XXXX, XXX, XXX−XXX

Scheme 7. Optimized Conditions for Suzuki Coupling

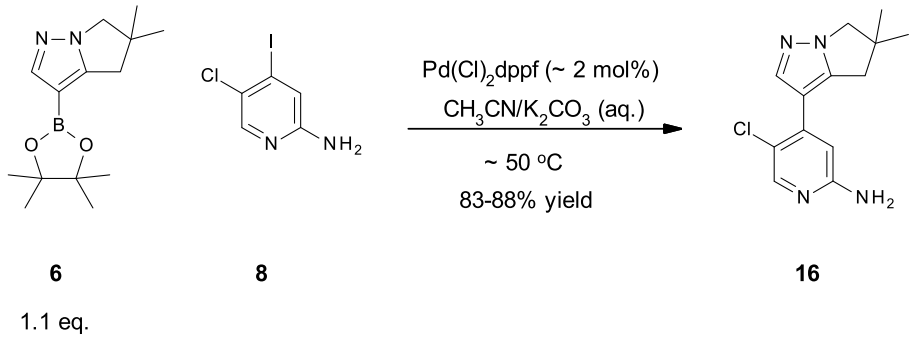

Scheme 8. Optimized Conditions for the Amide Coupling

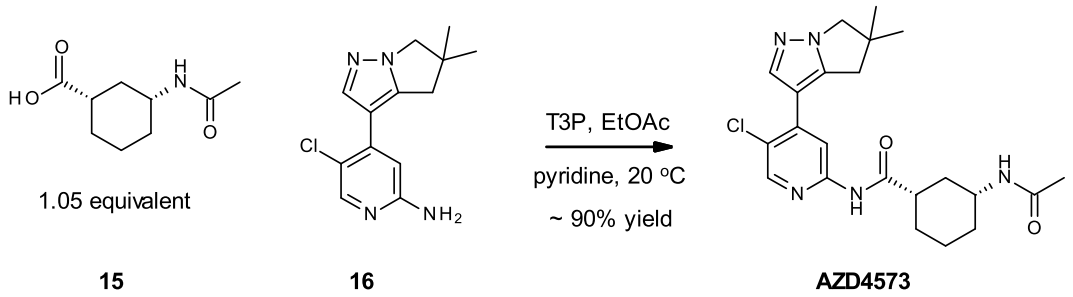

Scheme 9. Conditions for Multikilogram Manufacture of AZD4573

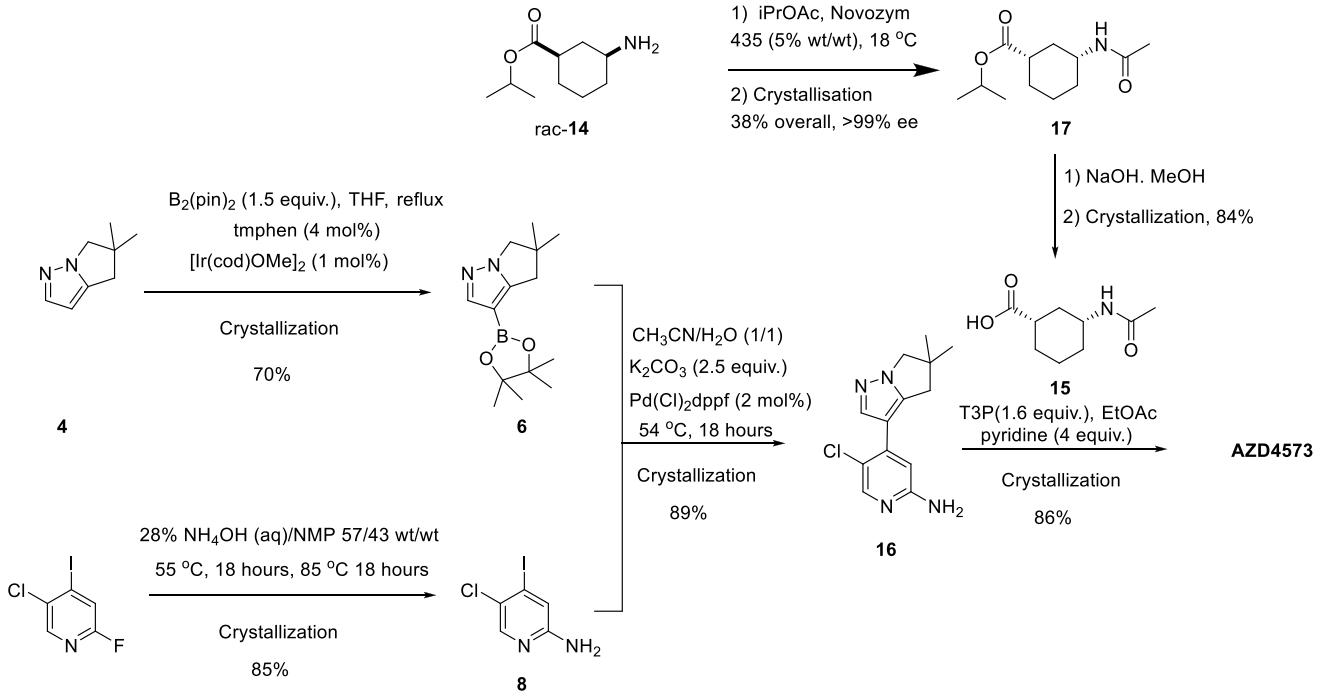

optimization. Fortunately, a ^{1}H NMR spectrum recorded in $CDCl_3$ of the crude mixture showed well resolved peaks for the two reactants **6** and **8** as well as for the expected byproduct **4** resulting from a protodeborylation of the pinacole ester **6** (Figure 6).

Surprisingly, we did not observe any byproduct resulting from reductive dehalogenation of the iodo-starting material **8**.[14] On the other hand, we noted that, after prolonged heating, the starting boronate **6** underwent proto-deborylation resulting in byproduct **4**. Fortunately, this side-reaction seemed to be significantly slower than the rate of the desired reaction. Therefore, we suspected that a large excess of the boronate **6** probably was not required. We performed a few control experiments to verify this hypothesis and found that as anticipated, only a slight excess of boronate **6** was required to reach full conversion of iodide **8**. Using optimal conditions, we chose to use 1.1 equiv of the boronate **6** which resulted in a good assayed yield of product **16** (Scheme 7). After a quick screen of solvents and bases for the reaction, we found that aqueous CH_3CN in combination with K_2CO_3 gave equal or better results

https://doi.org/10.1021/acs.oprd.1c00058
Org. Process Res. Dev. XXXX, XXX, XXX−XXX

compared with dioxane/K_2HPO_4 used in the first generation synthesis and was chosen as the preferred method for large scale manufacture of **16**. The catalyst $Pd(Cl)_2$dppf was selected due to accessibility and low cost.

Next, a straightforward and robust workup procedure was established. We chose to perform a direct extractive workup with EtOAc and aqueous washes. In the manufacture of the preclinical material, to minimize risk of contamination of API with palladium to an unacceptable level, we chose to add a Si-thiol scavenger at this stage to remove the major part of the palladium content. We believed that two subsequent crystallizations further downstream in the sequence would be enough to reach acceptable levels of palladium. Crude product **16** after treatment with scavenger followed by concentration was obtained as a highly discolored solid in quantitative assayed yield. After a screen of solvents for crystallization/slurrying of the crude product, we eventually found that the discoloration was efficiently removed after slurrying in methylisobutylketone (MIBK). On a 50−100 g scale, the desired product **16** was obtained as a colorless solid in 83% isolated yield with 100% assay (w/w) by ^{1}H NMR. By further optimization of the workup procedure above, we found that a direct crystallization of **16** was possible after basification of an acidic aqueous solution of **16** and no MIBK slurrying operation was necessary. Also, for the following large scale campaign, we decided to exclude the use of the Si-thiol scavenger from this reaction step and implement that operation after the final reaction step instead.

Optimization of Amide Coupling. For reasons of limited availability and nontrivial handling on a large scale, we searched for alternatives to Ghosez coupling reagent used in the first generation synthesis. We quickly found that propylphosphonic anhydride (T3P) efficiently mediated the coupling of carboxylic acid **15** with amine **16** and this reagent was also easy to handle, being sourced as a 50% solution in EtOAc (Scheme 8).

On a 50 g scale using an almost equimolar ratio of carboxylic acid **15** and amine **16** and using pyridine as the base, a 99% crude assayed yield of **AZD4573** was obtained after an extractive workup. We found that slurrying the crude product in CH_3CN finally gave the desired polymorph of **AZD4573** in 90% yield and with better than 98% assay (w/w) by ^{1}H NMR. Chiral HPLC analysis showed better than 99% ee and the concentration of palladium was at an acceptable level of <10 ppm. For the following multikilogram campaign, we found that a solvent swap from EtOAc to MIBK resulted in crystallization of the desired polymorph of **AZD4573** and a separate crystallization step in CH_3CN was not necessary.

Multikilogram Manufacture of AZD4573. For the multikilogram manufacture of **AZD4573** to support the clinical studies, the optimized conditions described in Scheme 9 were used.

The iridium-catalyzed borylation of **4**[15] proceeded non-eventfully using 1 mol % of the catalyst, 4 mol % of the phenanthroline ligand, and 1.5 equiv of the $B_2(pin)_2$ boron source. These were the same conditions as identified from the original high-throughput screening work, which had been found to work well with no need for further optimization. In order to achieve some level of consistency with the original glovebox screening conditions (<5 ppm of O_2), the oxygen level in the headspace was maintained below 5000 ppm by implementing several nitrogen-vacuum cycles. To remove most discoloration and insoluble impurities that were found to inhibit the crystallization of **6**, the workup consisted of treatment with activated carbon followed by filtration through a short bed of silica gel. Subsequently, after a solvent switch from the THF solution of **6** into MeOH and water, the desired product **6** crystallized and was isolated by filtration. In order to obtain an acceptable purity, we found it necessary to redissolve the product in warm heptane followed by filtration which removed additional insoluble impurities. After cooling the filtrate, the suspension formed was then filtered to afford 5.6 kg of boronate **6** (70% yield) as an off-white solid of high purity (99% purity by HPLC; 99 wt %/wt assay by NMR). The workup and isolation procedures employed here to obtain **6** were quite time-consuming and required a large amount of organic solvent (in total about 30 relative volumes of MeOH/heptane were used), so improving this workup will be a focus for process design ahead of future manufacturing campaigns. However, in comparison with the previously employed multistep bromination/lithium−halogen exchange/boronate quench sequence described above, requiring both nonenvironmentally benign solvents such as CH_2Cl_2 and cryogenic conditions, an overall improvement in process mass intensity (PMI), environmental sustainability, and ease of operations has been accomplished by developing the Ir-catalyzed borylation conditions for this transformation.

As described further above in more detail, ammonolysis of the 2-fluoropyridine **7** to provide **8** could be performed safely and with good yield on multikilogram scale. After an extractive workup using MTBE as the organic solvent, a solvent swap to toluene enabled crystallization and the desired compound **8** was isolated by filtration as a colorless solid (4.13 kg; 85% yield; 100 wt %/wt assay by NMR).

The Suzuki coupling of **6** and **8** using a 2 mol % loading of the $Pd(Cl)_2$dppf catalyst proceeded cleanly, and an extractive workup using EtOAc as the organic solvent left the desired compound in the organic layer. To facilitate the subsequent crystallization and to remove most of the impurities originating from the catalyst, the product was extracted into an acidic aqueous layer followed by basification, before addition of MeOH to affect crystallization. As stated above, the previously employed Si-thiol scavenger was removed from this step, to be introduced subsequently at the API stage. The desired product **16** was isolated as a colorless solid on a multikilogram scale by filtration (89% yield; 100 wt %/wt assay by NMR). ICP-OES analysis was performed and showed residual B, Ir, and Pd of 5.40, 67.4, and 638 ppm, respectively.

The enantiomerically pure amido-ester **17** was obtained on multikilogram scale after a resolution of the racemic cis-configured **14** using a 5 weight% loading of Novozym 435 as catalyst followed by crystallization (38% yield; >99% purity, HPLC; >99% ee, HPLC). Compound **15** was then obtained by hydrolysis of **17** using sodium hydroxide and subsequent isolation by crystallization in 84% overall yield with excellent purity (100% purity, HPLC; 100% ee, HPLC; 99 wt %/wt assay by NMR).

Finally, the coupling of building blocks **15** and **16** using the optimized conditions described in Scheme 9 gave crude **AZD4573** after a simple extractive workup. To remove residual palladium and iridium from the previous step, we chose to apply an immobilized metal scavenger (3-mercaptopropyl ethylsulfide silica). This was followed by final crystallization from MIBK to give 3.96 kg of **AZD4573** (86% yield; 98 wt %/wt assay by NMR; 99.9% chemical purity by HPLC; >99.5% ee by HPLC). Residual B, Ir, and Pd were at acceptable levels below 5 ppm (ICP-OES).

https://doi.org/10.1021/acs.oprd.1c00058
Org. Process Res. Dev. XXXX, XXX, XXX−XXX

CONCLUSION

Using the first generation mg-scale synthesis of **AZD4573** as a starting point, we have applied a focused combination of route design and process development to rapidly generate a much more scalable and efficient route, enabling multigram manufacture of API for use in preclinical studies. This second generation synthetic route was further modified, and the steps were optimized to give a third generation synthesis which was successfully used in the multikilogram scale manufacture of API to support initial clinical studies. With the primary focus being to develop a manufacturing route which is safe and easy to operate, with better environmental sustainability, we have made significant improvements along the way such as (i) reduced overall step count (6 steps vs 9 steps for third generation vs first generation); (ii) replacement of all chromatographic purifications with crystallizations; (iii) elimination of all chlorinated solvents; (iv) clear demonstration that the hazardous Wolff–Kishner reduction could potentially be replaced with a palladium-catalyzed hydrogenation; and (v) extensive use of catalytic transformations, including development of an enzymatic resolution/acetylation of a racemic amino-ester to afford access to a homochiral amido acid and replacement of a cryogenic two-step borylation sequence with a direct iridium-catalyzed borylation.

EXPERIMENTAL SECTION

All reactions were performed under an atmosphere of nitrogen. Reagents were commercially available and used without further purification. ^{1}H and ^{13}C NMR were recorded on a Bruker Avance III spectrometer at 25 °C at the frequency stated in each experiment. The chemical shifts (δ) are reported in parts per million (ppm), with the residual solvent signal used as a reference. Coupling constants (J) are reported as Hz. NMR abbreviations are used as follows: br = broad, s = singlet, d = doublet, t = triplet, q = quartet, m = multiplet. The strength/assay of intermediates and final products are given as weight/weight (w/w) and were determined by ^{1}H NMR measurements using benzyl benzoate, maleic acid, 1,3,5-trimethoxybenzene, or 1,2,4,5-tetrachloro-3-nitrobenzene (TCNB) as internal standards. In the iridium catalyzed borylation screen, the following instrument and conditions were used for determination of conversion of **4** to **6**: UPLC/MS using a Phenomenex Kinetex 2.6 μm C18 100A 75 mm × 3 mm column + guard column, 220 nm, 40 °C. A = 0.1% (w/v) NH_4Ac/H_2O, B = 0.1% (w/v) NH_4Ac/MeCN, gradient 5−95% B over 4 min, 95% B 0.5 min, 1.2 mL/min, 3 μL injection volume. The UHPLC/MS analyses were performed using a Waters Acquity UPLC system combined with a Waters SQD Mass Spectrometer. The UHPLC was equipped with both a BEH 1.7 μm C18 column 2.1 mm × 50 mm using a 46 mM ammonium carbonate/NH_3 buffer at pH 10 as eluent or an HSS 1.8 μm C18 column 2.1 mm × 50 mm using an 11 mM ammonium formate buffer at pH 3 as eluent. The mass spectrometer was operated with electrospray ionization (ESI) in both positive and negative mode. The enantiomeric excess of the corresponding isopropylester of **15** was determined by analytical SFC [Lux C2 column (4.6 mm × 150 mm), 15% 2-propanol in CO_2, 120 bar, as eluent]. HRMS measurements were performed on a QTOF 6530 instrument (Agilent), mass precision ±5 ppm.

3-Bromo-5,5-dimethyl-5,6-dihydro-4*H*-pyrrolo[1,2-*b*]-pyrazole (5a). In a 1 L reactor under an atmosphere of nitrogen were charged 5,5-dimethyl-5,6-dihydro-4*H*-pyrrolo[1,2-*b*]-pyrazole **4** (79.5 g, 90 wt %/wt, 525 mmol) and CH_2Cl_2 (800 mL). With a jacket temperature of +10 °C, to the homogeneous yellow solution was added portionwise 1-bromopyrrolidine-2,5-dione (95.4 g, 533 mmol) during 15 min. The reaction temperature was kept in the interval +20 to +23 °C during this addition. A solution of 8% Na_2SO_3 (aq., 250 mL) was added, and the biphasic mixture was stirred for 45 min. The organic layer was washed with Na_2CO_3 solution (aq. sat., 2 × 250 mL) and last water (100 mL) followed by careful concentration at 30 °C and 400 mbar. Residual water was azeotropically removed using THF (3 × 100 mL). This afforded the title compound **5a** as a pale brown oil (138 g, 81 wt %/wt, 520 mmol, 99% yield) with THF as the major impurity. Analytical data were in accordance with those given in literature.[3]

5,5-Dimethyl-3-(4,4,5,5-tetramethyl-1,3,2-dioxaborolan-2-yl)-5,6-dihydro-4*H*-pyrrolo[1,2-*b*]pyrazole (6) via Lithiation/Triisopropylborate Quench. Under an atmosphere of nitrogen and in a 3 L three-necked flask equipped with a thermometer, to a −70 °C solution of 3-bromo-5,5-dimethyl-5,6-dihydro-4*H*-pyrrolo[1,2-*b*]pyrazole **5a** (137 g, 81 wt %/wt, 516 mmol) and triisopropyl borate (175 g, 929 mmol) in THF (0.7 L) and toluene (0.7 L) was slowly (80 min) added a solution of butyllithium (2.5 M in hexanes, 0.309 L, 772 mmol) while maintaining the reaction temperature in the interval −65 °C to −70 °C. ^{1}H NMR analysis of the crude mixture showed full conversion to the intermediate *i*-Pr-borate **13**. At −70 °C, a solution of 2,3-dimethylbutane-2,3-diol (91 g, 774 mmol) dissolved in toluene (0.5 L) was added during 10 min. The mixture was slowly allowed to attain 20 °C in the ice bath and was then stirred for an additional 16 h. A pale brown homogeneous solution was obtained. ^{1}H NMR analysis of the crude mixture showed full conversion of **13** to **6**. The reaction mixture was transferred to a 5 L reactor containing a 10 °C solution of NH_4Cl (aq., sat, 2.5 L). The biphasic mixture was stirred for 15 min at 20 °C. The organic layer was washed with water (2 × 500 mL) followed by concentration under reduced pressure at 35 °C to a pale yellow wax-solid **6** (193.6 g, 64 wt %/wt, 473 mmol, 92% yield) with toluene and pinacole as major impurities. Analytical data were in accordance with those given in the literature.[3]

5,5-Dimethyl-3-(4,4,5,5-tetramethyl-1,3,2-dioxaborolan-2-yl)-5,6-dihydro-4*H*-pyrrolo[1,2-*b*]pyrazole (6) via Iridium Catalyzed Borylation. 5,5-Dimethyl-4,6-dihydropyrrolo[1,2-*b*]pyrazole (**4**, 4.1 kg, 30.1 mol) and dry THF (36.5 kg, ≤ 0.05% H_2O wt/wt) were charged into a 80 L glass reactor. Bis (pinacolato) diboron (11.5 kg, 45.3 mol) and 3,4,7,8-tetramethyl-1,10-phenanthroline (0.29 kg, 1.2 mol) were added, and the solution was then stirred for 1 h at 15−25 °C. The mixture was evacuated to $P \leq -0.08$ MPa and then filled with nitrogen to normal pressure. This operation was repeated 5 times until the oxygen content was ≤5000 ppm. Bis [cyclooctadiene(methoxy)iridium] (0.20 kg, 0.30 mol) was added, and the mixture was evacuated to $P \leq -0.08$ MPa and then filled with nitrogen to normal pressure. This operation was repeated 5 times until the oxygen content was ≤5000 ppm. The mixture was heated to 70−80 °C and then stirred for 12 h. The reaction mixture was cooled to 20 °C. Active charcoal (0.41 kg) was added in two portions, and the mixture was then heated to 45 °C and stirred for 3 h. The mixture was filtered using a 10 L vacuum filter flask which was preloaded with Silica gel (2 cm bed, 0.5 kg, 200−300 mesh). The filter cake was rinsed twice with THF (7.3 kg +7.3 kg). The filtrates were combined and concentrated at ≤45 °C under reduced pressure ($P \leq -0.08$ MPa). While the

https://doi.org/10.1021/acs.oprd.1c00058
Org. Process Res. Dev. XXXX, XXX, XXX−XXX

temperature was maintained at ≤45 °C, methanol (6.3 kg) was added, and the mixture was stirred for 3 h followed by concentration at ≤45 °C under reduced pressure ($P \leq -0.08$ MPa). Methanol (6.5 kg) was again added, and the procedure above was repeated twice. Then the mixture was cooled to 20 °C. Water (40.9 kg) was added, and the suspension formed was stirred for 3 h followed by filtration. Methanol (3.7 kg) and the filter cake were added into the reactor at 20 °C and then stirred for 1 h. Water (41.1 kg) was added, and the mixture was stirred for 3 h followed by filtration. The filter cake was charged to the reactor, and *n*-heptane (70 kg) was added followed by heating to 50 °C and stirring for 3 h. The mixture was filtered, and the filtrate was concentrated at 55 °C under reduced pressure $P \leq -0.08$ MPa until 14 L of the content remained. The mixture was cooled to 0 °C and was stirred for 4 h followed by filtration and washing of the filter cake with ice-cold *n*-heptane (1.4 kg × 2) and last water (4.1 kg + 4.0 kg). The cake was dried at 30 °C under vacuum to give the title compound **6** as an off-white solid (5.6 kg, 99 wt %/wt, 21.1 mol, 70% yield). ^{1}H NMR (500 MHz, $CDCl_3$) δ 1.28 (s, 6H); 1.29 (s, 12H); 2.79 (s, 2H); 3.86 (s, 2H); 7.76 (s, 1H). ^{13}C NMR (126 MHz, $CDCl_3$) δ 25.0 (4 Cs), 28.5 (2 Cs), 39.3, 43.3, 61.0, 83.0 (2 Cs), 100.3 (br), 149.5, 153.0. HRMS $[M + H]^+$ m/z calcd for $C_{14}H_{24}BN_2O_2$ 263.1925, found 263.1935.

5-Chloro-4-iodo-pyridin-2-amine (8). An aqueous solution of ammonium hydroxide (28 wt %/wt, 12.6 kg, 101 mol) was added to a well agitated nitrogen purged C22 hastelloy pressure reactor followed by line rinsing with water (2 kg). At a temperature of 13 °C, 5-chloro-2-fluoro-4-iodopyridine (4.915 kg, 19.1 mol) dissolved in NMP (8 kg) was slowly added during 10 min (slightly exothermic) followed by line rinsing with NMP (3.2 kg). The reaction temperature was maintained below 20 °C during this addition. The reactor was sealed, and the internal temperature was increased to 55 °C which resulted in an internal pressure of 1.78 barg. The mixture was stirred for 18 h which resulted in an 83% conversion of the starting fluoropyridine (internal pressure 1.41 barg). The reaction mixture was heated to 85 °C (internal pressure 3.9 barg) and was stirred for an additional 18 h followed by cooling to ambient temperature. MTBE (20.3 kg) was added followed by the addition of water (10.8 kg). The aqueous layer was extracted with MTBE (13.7 L × 2), and the combined organic layer was washed with water (9.5 L × 3). Toluene (10 L) was added, and the jacket temperature was increased to 110−130 °C to distill off most of the MTBE. Toluene (10 L) was again added, and distillation continued until a total of 70 L of the volatiles had been distilled off. The reaction mixture was then slowly cooled to 2 °C during 4 h and was stirred at that temperature for an additional 18 h followed by filtration of the suspension and washing of the filter cake with toluene (2 L × 2). The cake was then dried under vacuum at 40 °C to give the title compound **8** as a colorless solid (4.13 kg, 100 wt %/wt, 16.2 mol, 85% yield). Analytical data were in accordance with those of commercial authentic material.

5-Chloro-4-(5,5-dimethyl-4,6-dihydropyrrolo[1,2-*b*]-pyrazol-3-yl)pyridin-2-amine (16). Compound **8** (3.03 kg, 11.9 mol) was charged to a reactor followed by water (25.3 L), compound **6** (3.58 kg, 13.4 mol), and last CH_3CN (25.3 L). The vessel was degassed by using vacuum/nitrogen purge. Potassium carbonate (4.11 kg, 29.7 mol) was added followed by [1,1′-bis(diphenylphosphino)ferrocene]dichloropalladium(II) (174 g, 0.24 mol). The two-phase mixture was stirred vigorously at 54 °C for 18 h followed by cooling to 20 °C. EtOAc (22.8 L) was added followed by separation of the phases. The organic phase was washed twice with a solution of NaCl (1.02 kg) in water (9.1 kg) and then sequentially extracted with an aqueous solution of HCl (2M, 15 L, 10.5 L, 10.5 L). The combined three aqueous layers were transferred back to the reactor via an in-line filter (5 μm), and MeOH (10 L) was added followed by careful pH adjustment to 11 using a 45% aqueous solution of KOH (16.36 kg, 131.3 mol) while maintaining the temperature below 30 °C. The mixture was then stirred at 20 °C for 1 h followed by filtration and washing of the filter cake with water (6 L). The cake was then dried at 50 °C under vacuum to give the title compound **16** as a colorless solid (2.76 kg, 100 wt %/wt, 10.5 mol, 88% yield). ICP-OES analysis showed residual B, Ir, and Pd of 5.40, 67.4, and 638 ppm, respectively. ^{1}H NMR (500 MHz, $CDCl_3$) δ 1.32 (6H, s); 2.85 (2H, s); 3.94 (2H, s); 4.41 (2H, s, br); 6.44 (s, 1H); 7.85 (s, 1H), 8.06 (s, 1H). ^{13}C NMR (126 MHz, $CDCl_3$) δ 28.1, 40.5, 43.5, 61.1, 107.8, 112.0, 119.3, 141.3, 142.8, 144.1, 148.1, 157.0. HRMS $[M + H]^+$ m/z calcd for $C_{13}H_{16}ClN_4$ 263.1058, found 263.1066.

(1*S*,3*R*)-3-Acetamidocyclohexanecarboxylic Acid (15). *Resolution of Enantiomers rac-**14**.* A reactor was charged with compound *rac*-**14** (16.8 kg, 90.7 mol) and *i*-PrOAc (132 L). The reaction temperature was kept at 18 °C, and Candida Antarctica lipase B (839 g, 5 wt %) was added. The mixture was stirred for at least 13 h until a conversion of 48% of *rac*-**14** had been obtained. The mixture was centrifuged, and the cake was washed with *i*-PrOAc (16.8 L × 2). The filtrate was collected and transferred back to the reactor. A solution of oxalic acid dihydrate (2.85 kg, 22.6 mol) in water (50.3 L) was added to the reactor at 20 °C. The mixture was kept at that temperature and stirred for 1 h followed by separation of phases. The aqueous phase was extracted with *i*-PrOAc (50.3 L), and the combined organic layers were washed with water (16.8 L) and brine (83.9 L, 35 wt %) followed by concentration under vacuum $P \leq -0.08$ MPa at 40 °C until the concentration of product is 3.0 relative volumes. Cyclopentylmethyl ether (CPME, 42.0 L) was added, and the mixture was concentrated under vacuum $P \leq -0.08$ MPa at 40 °C until 3 relative volumes of solvent remained. The procedure was repeated three times until the content of *i*-PrOAc was 3%. Cyclohexane (154.4 L) was added (CPME content = 25%). The mixture was heated to 60 °C and kept at that temperature for 0.5 h. The clear homogeneous solution was cooled to 50 °C in 2 h and kept at that temperature for 1 h. The mixture was cooled to 40 °C in 2 h and kept at that temperature for 1 h. The mixture was cooled to 30 °C in 2 h and kept at that temperature for 1 h. The mixture was then finally cooled to 20 °C in 2 h and stirred for an additional 12 h. The suspension was centrifuged, and the cake was washed with cyclohexane/CPME = 5/1 (16.8 L × 2). The cake was dried in an oven under $P \leq -0.08$ MPa at 40 °C for 6 h to give the desired amido-ester **17** (7.88 kg, 38.3% yield) with 99.7% chemical purity and ee 99.9%. Analytical data were in accordance with those reported previously.[13]

*Hydrolysis To Give **15**.* At 20 °C, to a reactor containing water (39.7 L), NaOH (2.05 kg, 51.3 mol), and MeOH (28.0 L) was added in portions the above amidoester (7.78 kg, 34.2 mol). The mixture was stirred at 25 °C for 3 h followed by the addition of water (54.5 L). The mixture was concentrated under vacuum $P \leq -0.08$ MPa at ≤40 °C until the solution was not more than 9.0 relative volumes and the MeOH content = 7%. Sodium chloride (14.8 kg, 253.3 mol) was added and the mixture was stirred for 1 h. The reactor content was filtered through a fluid filter membrane followed by washing with water (0.5 relative volumes). The mixture was cooled to 15 °C and a concentrated

https://doi.org/10.1021/acs.oprd.1c00058
Org. Process Res. Dev. XXXX, XXX, XXX−XXX

aqueous solution of HCl was added dropwise until pH ≤ 1. The suspension formed was stirred for an additional 0.5 h followed by centrifugation and washing of the cake with water (7.8 L × 2). After drying of the solid under vacuum $P \leq -0.08$ MPa at 40 °C for 6 h, the desired compound **15** (5.39 kg, 29.1 mol) was obtained in 100% chemical purity by HPLC (assay 99 wt %/wt by 1H NMR), ee > 99.5%. Other analytical data were in accordance with those reported previously.[13]

(1*S*,3*R*)-3-Acetamido-*N*-[5-chloro-4-(5,5-dimethyl-4,6-dihydropyrrolo[1,2-*b*]pyrazol-3-yl)-2-pyridyl]cyclohexanecarboxamide (AZD4573). Compound **16** (2.758 kg, 10.50 mol) and EtOAc (27 L) were charged to the reactor followed by the addition of **15** (2.041 kg, 10.80 mol) and pyridine (3.39 L, 41.9 mol). 1-Propanephosphonic anhydride (T_3P, 50% in EtOAc, 10.01 kg, 17.0 mol) was added during 20 min maintaining the reaction temperature below +23 °C. The mixture was stirred at 20 °C for 18 h followed by the addition of water (19.5 L) during 10 min. The mixture was stirred for 25 min at 20 °C followed by separation of the phases. The aqueous phase was extracted with EtOAc (13.7 L), and the combined organic layers were washed with a solution of K_2CO_3 (1.407 kg, 10.18 mol) in water (11.17 kg). The organic layer was washed with water (13 L × 2) followed by the addition of 3-mercaptopropyl ethyl sulfide silica (1.32 kg, 60−200 mesh). The mixture was stirred at 20 °C for 18 h followed by filtration of the suspension and rinsing with EtOAc (7 L × 2). The organic layer was charged to the reactor via an in-line filter (1 μm), and the volatiles were distilled off at 70 °C until a total volume of 27.6 L was obtained. Methylisobytyl ketone (MIBK, 27.5 L) was added followed by removal of 20 L of the volatiles through distillation. More MIBK (27.5 L) was added followed by distilling off 16 L of the volatiles. More MIBK (13.75 L) was added followed by removal of 13.5 L of the volatiles through distillation. This procedure was repeated one more time. The temperature of the mixture was cooled to 105 °C, and seeds of correct polymorph (3.6 g) of **AZD4573** were added followed by stirring for 1 h. The suspension was then cooled to 20 °C at 0.2 °C/min and stirred for 1 h. A temperature cycling program was applied: heating to 40 °C followed by stirring for 1 h and then cool mixture to 20 °C again and stir for 1 h. This procedure was repeated 3 times. The suspension was then stirred at 20 °C for 18 h followed by cooling to 10 °C and stirring for an additional 1 h. The mixture was filtered, and the cake washed with MIBK (4.5 L × 3) followed by drying under vacuum at 70 °C to give the title compound **AZD4573** as colorless crystals (3.96 kg, 98 wt %/wt by NMR, 99.9% purity by HPLC, 9.0 mol, 86% yield). ICP-OES analysis showed levels of B, Ir, and Pd below 5 ppm. HRMS $[M + H]^+$ m/z calcd for $C_{22}H_{29}ClN_5O_2$ 430.2004, found 430.2009, ee > 99.5% by HPLC. NMR data were in agreement with those recently reported.[3]

■ ASSOCIATED CONTENT

Supporting Information

The Supporting Information is available free of charge at https://pubs.acs.org/doi/10.1021/acs.oprd.1c00058.

^{1}H NMR, ^{13}C NMR, HPLC chromatograms for intermediates and **AZD4573**, screening results for Ir-catalyzed borylation of **4**. Analytical testing report for compound **15**. Experimental procedures for preparation of compounds **2**, **3**, **4** (PDF)

■ AUTHOR INFORMATION

Corresponding Author

Staffan Karlsson − *Early Chemical Development, Pharmaceutical Sciences, Biopharmaceuticals R&D, AstraZeneca, Gothenburg, Sweden*; orcid.org/0000-0002-5302-7157; Email: staffan.po.karlsson@astrazeneca.com

Authors

Helen Benson − *Early Chemical Development, Pharmaceutical Sciences, Biopharmaceuticals R&D, AstraZeneca, Macclesfield, United Kingdom*

Calum Cook − *Early Chemical Development, Pharmaceutical Sciences, Biopharmaceuticals R&D, AstraZeneca, Macclesfield, United Kingdom*

Gordon Currie − *Early Chemical Development, Pharmaceutical Sciences, Biopharmaceuticals R&D, AstraZeneca, Macclesfield, United Kingdom*

Jerome Dubiez − *Early Chemical Development, Pharmaceutical Sciences, Biopharmaceuticals R&D, AstraZeneca, Macclesfield, United Kingdom*

Hans Emtenäs − *Early Chemical Development, Pharmaceutical Sciences, Biopharmaceuticals R&D, AstraZeneca, Gothenburg, Sweden*

Janet Hawkins − *Medicinal Chemistry, Oncology R&D, AstraZeneca, Cambridge, United Kingdom*

Rebecca Meadows − *Chemical Development, Pharmaceutical Technology & Development, Operations, AstraZeneca, Macclesfield, United Kingdom*

Peter D. Smith − *Early Chemical Development, Pharmaceutical Sciences, Biopharmaceuticals R&D, AstraZeneca, Macclesfield, United Kingdom*; orcid.org/0000-0001-5312-9893

Jeffrey Varnes − *Medicinal Chemistry, Oncology R&D, AstraZeneca, Boston, Massachusetts 02451, United States*

Complete contact information is available at: https://pubs.acs.org/10.1021/acs.oprd.1c00058

Notes

The authors declare no competing financial interest.

■ ACKNOWLEDGMENTS

We thank Steven McKown (Early Chemical Development, Pharmaceutical Sciences, AstraZeneca), Trevor Churchill (Global Process Safety, Pharmaceutical Technology & Development, AstraZeneca), Danny Mortimer (Johnson-Matthey Catalysis and Chiral Technologies, Cambridge, U.K.), Chris Atherton (Onyx Scientific Ltd, Sunderland, U.K.), Jianbo Yang et al. (Asymchem Laboratories, Tianjin, China), and Liao Xiaoming et al. (Pharmaron, Beijing, China) for their contributions to this work.

■ ABBREVIATIONS

TLC, thin layer chromatography
DMA, Dimethylacetamide
NBS, *N*-Bromosuccinimide
NIS, *N*-Iodosuccinimide
DIPEA, Diisopropylethylamine
Ghosez reagent, 1-Chloro-*N*,*N*-2-trimethyl-1-propenylamine
MsOH, Methanesulfonic acid
TFA, Trifluoroacetic acid
PFA, Perfluoroalkoxy
API, Active Pharmaceutical Ingredient
DSC, Differential Scanning Calometry

https://doi.org/10.1021/acs.oprd.1c00058
Org. Process Res. Dev. XXXX, XXX, XXX−XXX

PMI, Process Mass Intensity
ICP-OES, Inductively Coupled Plasma Optical Emission Spectroscopy

REFERENCES

(1) For example see: (a) Sonawane, Y. A.; Taylor, M. A.; Napoleon, J. V.; Rana, S.; Contreras, J. I.; Natarajan, A. Cyclin Dependent Kinase 9 Inhibitors for Cancer Therapy. *J. Med. Chem.* **2016**, *59*, 8667−8684. (b) Wang, S.; Griffiths, G.; Midgley, C. A.; Barnett, A. L.; Cooper, M.; Grabarek, J.; Ingram, L.; Jackson, W.; Kontopidis, G.; McClue, S. J.; McInnes, C.; McLachlan, J.; Meades, C.; Mezna, M.; Stuart, I.; Thomas, M. P.; Zheleva, D. I.; Lane, D. P.; Jackson, R. C.; Glover, D. M.; Blake, D. G.; Fischer, P. M. Discovery and characterization of 2-anilino-4-(thiazol-5-yl)pyrimidine transcriptional CDK inhibitors as anticancer agents. *Chem. Biol.* **2010**, *17*, 1111−1121.

(2) (a) Booher, R. N.; Hatch, H.; Dolinski, B. M.; Nguyen, T.; Harmonay, L.; Al-Assaad, A.-S.; Ayers, M.; Nebozhyn, M.; Loboda, A.; Hirsch, H. A.; Zhang, T.; Shi, B.; Merkel, C. E.; Angagaw, M. H.; Wang, Y.; Long, B. J.; Lennon, X. Q.; Miselis, N.; Pucci, V.; Monahan, J. W.; Lee, J.; Kondic, A. G.; Im, E. K.; Mauro, D.; Blanchard, R.; Gilliland, G.; Fawell, S. E.; Zawel, L.; Schuller, A. G.; Strack, P. MCL1 and BCL-xL Levels in Solid Tumors Are Predictive of Dinaciclib-Induced Apoptosis. *PLoS One* **2014**, *9*, e108371. (b) Cidado, J.; Boiko, S.; Proia, T.; Ferguson, D.; Criscione, S. W.; San, M. M.; Pop-Damkov, P.; Su, N.; Roamio, F. V. N.; Sekhar, R. C. C.; D'Santos, C. S.; Shao, W.; Saeh, J. C.; Koch, R.; Weinstock, D. M.; Zinda, M.; Fawell, S. E.; Drew, L. AZD4573 Is a Highly Selective CDK9 Inhibitor That Suppresses MCL-1 and Induces Apoptosis in Hematologic Cancer Cells. *Clin. Cancer Res.* **2020**, *26*, 922−934.

(3) Barlaam, B.; Casella, R.; Cidado, J.; Cook, C.; De Savi, C.; Dishington, A.; Donald, C. S.; Drew, L.; Ferguson, A. D.; Ferguson, D.; Glossop, S.; Grebe, T.; Gu, C.; Hande, S.; Hawkins, J.; Hird, A. W.; Holmes, J.; Horstick, J.; Jiang, Y.; Lamb, M. L.; McGuire, T.; Moore, J. E.; O'Connell, N.; Pike, A.; Pike, K. G.; Proia, T.; Roberts, B.; Martin, M. S.; Sarkar, U.; Shao, W.; Stead, D.; Sumner, N.; Thakur, K.; Vasbinder, M. M.; Varnes, J. G.; Wang, J.; Wang, L.; Wu, D.; Wu, L.; Yang, B.; Yao, T. Discovery of AZD4573, a potent and selective inhibitor of CDK9 that enables short duration of target engagement for the treatment of hematological malignancies. *J. Med. Chem.* **2020**, *63*, 15564−15590.

(4) Galeta, J.; Tenora, L.; Man, S.; Potácek, M. Dihydropyrrolo[1,2-b]pyrazoles: withasomnine and related compounds. *Tetrahedron* **2013**, *69*, 7139−7146.

(5) Amorín, M.; Castedo, L.; Granja, J. R. Self-Assembled Peptide Tubelets with 7 Å Pores. *Chem. - Eur. J.* **2005**, *11*, 6543−6551.

(6) (a) Stewart, G. W.; Brands, K. M. J.; Brewer, S. E.; Cowden, C. J.; Davies, A. J.; Edwards, J. S.; Gibson, A. W.; Hamilton, S. E.; Katz, J. D.; Keen, S. P.; Mullens, P. R.; Scott, J. P.; Wallace, D. J.; Wise, C. S. Process Development and Large-Scale Synthesis of a c-Met Kinase Inhibitor. *Org. Process Res. Dev.* **2010**, *14*, 849−858. (b) Newby, J. A.; Huck, L.; Blaylock, D. W.; Witt, P. M.; Ley, S. V.; Browne, D. L. Investigation of a Lithium−Halogen Exchange Flow Process for the Preparation of Boronates by Using a Cryo-Flow Reactor. *Chem. - Eur. J.* **2014**, *20*, 263−271 and references cited therein.

(7) Bottles of *n*-butyllithium were purchased from Aldrich and used freshly upon arrival. The molarity was assumed to be as specified on the label.

(8) Znidar, D.; O'Kearney-McMullan, A.; Munday, R.; Wiles, C.; Poechlauer, P.; Schmoelzer, C.; Dallinger, D.; Kappe, C. O. Scalable Wolff-Kishner Reductions in Extreme Process Windows Using a Silicon Carbide Flow Reactor. *Org. Process Res. Dev.* **2019**, *23*, 2445−2455.

(9) For example, see: (a) Sieser, J. E.; Maloney, M. T.; Chisowa, E.; Brenek, S. J.; Monfette, S.; Salisbury, J. J.; Do, N. M. Ir-Catalyzed Borylation as an Efficient Route to a Nicotine Hapten. *Org. Process Res. Dev.* **2018**, *22*, 527−534. (b) Campeau, L.-C.; Chen, Q.; Gauvreau, D.; Girardin, M.; Belyk, K.; Maligres, P.; Zhou, G.; Gu, C.; Zhang, W.; Tan, L.; O'Shea, P. D. A Robust Kilo-Scale Synthesis of Doravirine. *Org. Process Res. Dev.* **2016**, *20*, 1476−1481. (c) Larsen, M. A.; Hartwig, J. F. Iridium-Catalyzed C−H Borylation of Heteroarenes: Scope, Regioselectivity, Application to Late-Stage Functionalization, and Mechanism. *J. Am. Chem. Soc.* **2014**, *136*, 4287−4299.

(10) A recent publication describes the use of $Ca(EtCO_2)_2$ to efficiently remove HF formed: Blacker, A. J.; Malagon, G. M.; Powell, L.; Reynolds, W.; Stones, R.; Chapman, M. R. Development of an S_NAr Reaction: A Practical and Scalable Strategy to Sequester and Remove HF. *Org. Process Res. Dev.* **2018**, *22*, 1086−1091.

(11) Badland, M.; Bains, C. A.; Howard, R.; Laity, D.; Newman, S. D. An improved synthesis of (1R,3S)-3-[(tert-butoxycarbonyl)amino]-cyclohexanecarboxylic acid. *Tetrahedron: Asymmetry* **2010**, *21*, 864−866.

(12) (a) González-Sabín, J.; Gotor, V.; Rebolledo, F. Enantioselective acylation of rac-2-phenylcycloalkanamines catalyzed by lipases. *Tetrahedron: Asymmetry* **2005**, *16*, 3070−3076. (b) González-Sabín, J.; Gotor, V.; Rebolledo, F. Kinetic resolution of (±)-trans- and (±)-cis-2-phenylcyclopentanamine by CALB-catalyzed aminolysis of esters:the key role of the leaving group. *Tetrahedron: Asymmetry* **2004**, *15*, 481−488. (c) Gotor, V. Non-conventional hydrolase chemistry: amide and carbamate bond formation catalyzed by lipases. *Bioorg. Med. Chem.* **1999**, *7*, 2189−2197. (d) Skupinska, K. A.; McEachern, E. J.; Baird, I. R.; Skerlj, R. T.; Bridger, G. J. Enzymatic Resolution of Bicyclic 1-Heteroarylamines Using *Candida antarctica* Lipase B. *J. Org. Chem.* **2003**, *68*, 3546−3551. (e) González-Sabín, J.; Gotor, V.; Rebolledo, F. CAL-B-catalyzed resolution of some pharmacologically interesting *β*-substituted isopropylamines. *Tetrahedron: Asymmetry* **2002**, *13*, 1315−1320. (f) Choi, Y. K.; Kim, M. J.; Ahn, Y.; Kim, M.-J. Lipase/Palladium-Catalyzed Asymmetric Transformations of Ketoximes to Optically Active Amines. *Org. Lett.* **2001**, *3*, 4099−4101. (g) López-Serrano, P.; Jongejan, J. A.; van Rantwijk, F.; Sheldon, R. A. Enantioselective acylation of *α*-aminonitriles catalysed by *Candida antarctica* lipase. *Tetrahedron: Asymmetry* **2001**, *12*, 219−228. (h) Sánchez, V. M.; Rebolledo, F.; Gotor, V. *Candida antarctica* Lipase-Catalyzed Doubly Enantioselective Aminolysis Reactions. Chemoenzymatic Synthesis of 3-Hydroxypyrrolidines and 4-(Silyloxy)-2-oxopyrrolidines with Two Stereogenic Centers. *J. Org. Chem.* **1999**, *64*, 1464−1470.

(13) (a) Karlsson, S. Development of an Enantioselective Novozym 435 Mediated Acetylation for the Preparation of (1*S*,3*R*)-3-Acetamidocyclohexane-1-carboxylic Acid. *Org. Process Res. Dev.* **2016**, *20*, 1336−1340. (b) Pithani, S.; Karlsson, S.; Emtenäs, H.; Öberg, C. T. Using Spinchem Rotating Bed Reactor Technology for Immobilized Enzymatic Reactions: A Case Study. *Org. Process Res. Dev.* **2019**, *23*, 1926−1931.

(14) Using the bromo-analogue of **8** instead of iodo was attempted at an early stage of the route development, but this gave an unacceptable low yield of **16**.

(15) Building block **4** was obtained on multikilogram scale starting from pyrazole. Only minor modifications of the conditions in the first generation synthesis (Scheme 1) were used. Process descriptions can be found in the Supporting Information.

https://doi.org/10.1021/acs.oprd.1c00058
Org. Process Res. Dev. XXXX, XXX, XXX−XXX